# MONITORING COMMUNITY HYSTERESIS USING SPECTRAL SHIFT ANALYSIS AND THE RED-EDGE VEGETATION STRESS INDEX

Ray Merton
Department of Geography
University of Auckland
Private Bag, Auckland
New Zealand
*email*: r.merton@auckland.ac.nz

## 1. INTRODUCTION

The red-edge, centered at the largest change in reflectance per wavelength change, is located between two of the most widely used wavelength regions used for broad band vegetation studies, the red trough and the NIR plateau. The vegetation red-edge in Airborne Visible/Infrared Imaging Spectrometer (AVIRIS) data comprises eight contiguous spectral bands between 0.6852 - 0.7523μm.

The aim of this study focuses on the development of simple techniques to identify and model multi-temporal red-edge geometry changes in disparate vegetation communities at Jasper Ridge Biological Preserve, Palo Alto, California. This study examines the design and performance of selected measures for monitoring community stress from early spring to late autumn. Defining complex red-edge symmetry through a range of geometric and statistical measures has potential for seasonal and long-term vegetation monitoring.

Second-derivative calculations are applied to the measurement of red-edge inflection point shifts. Derivative spectra are also used to identify variations in red-edge geometry associated with apparent stress in communities and changing environmental variables and to determine bands for inclusion in the Red-edge Vegetation Stress Index (RVSI). Patterns of community hysteresis based on multi-temporal changes in spectral shifts, the RVSI, and other important vegetation indices are examined.

### 1.1 Vegetation Communities

Seven communities are selected to identify an environmental gradient that spans the mesic to near-xeric environments found in the Jasper Ridge Biological Preserve. By including a selection of disparate communities along this gradient, it is possible to more fully interpret spectral and multi-temporal trends. As ongoing research focuses on biogeochemical stress analysis, many communities located on Jasper Ridge retain the nomenclature representative of the underlying geology/soil (Merton, 1994).

The following is a brief description of communities. *Serpentine community*: restricted to the main serpentine deposit as a narrow-endemic tolerant of high geochemical toxicity and near-xeric conditions. Representative species include *Stipa pulchra* and *Eschscholzia californica*. *Sandstone community*: predominantly annual grassland species located on a sandstone substrate. Representative species include a range of annual grasses especially *Bromus rigidus*. *Halo community*: located in the moderate toxicity zone (geochemical halo) is influenced by mobile serpentine geochemicals. This distinctive community is regarded as an intermediate between the serpentine and sandstone communities. *Chaparral community*: a fire-climax community situated on dry southwest facing slopes containing chamise chaparral, *Prunus* chaparral, and *Baccharis* shrub. *Woodlands community*: an open canopy community situated predominantly on northwest slopes containing a range of oaks, buckeyes, and laurels. *Delta community*: a willow (*Salix lasiolepsis*) dominated community located in the swampy deltaic areas at the southern margin of Searsville Lake. *Redwood community*: dense stands of *Sequoia sempervirens* are located adjacent to San Francisquito Creek to the north of Jasper Ridge.

## 1.2 AVIRIS Datasets

Five AVIRIS datasets are selected to construct a near-consecutive multi-temporal database. Chronological five-date imagery is not available in any one year. Therefore, two spring datasets from 5 April 1996 and 30 April 1994 are combined with the consecutive 1992 datasets of 2 June, 1 September, and 6 October. Non-sequential datasets are substituted into the beginning of the series as spring is not normally associated with vegetation stress. This disparity between datasets, although not ideal, provides valuable indicator information of early season stress responses. Additionally, environmental variables such as precipitation and temperature did not vary significantly between dataset years. However, to reduce annual difference between datasets, environmental variables were recalculated as merged datasets combining data from intervals prior to image acquisition dates. The period between 2 June and 1 September is the largest with a 91 day interval. Ideally, another dataset in this period would provide additional information on summer trends.

# 2. METHODS

Eight band high spectral resolution (8.4nm FWHM) data encompassing the red-edge can be used to describe community phenological response through time as a function of changes to red-edge symmetry. Analyses such as Guyot (1992), focusing on the measurement of reflectance change, have endeavored to define the red-edge as a single quantifiable variable. My aim is to identify an appropriate single red-edge descriptor for vegetation stress analysis, defined not only by statistic techniques but by the identification and measurement of common red-edge geometric points.

## 2.1 Calculating Red-Edge Inflection From Second-Derivative Spectra

The red-edge is a relatively featureless waveform and does not display abrupt peaks or troughs between adjacent bands on which geometric analyses can be readily based. This section describes techniques for the calculation of red-edge inflection ($re_i$) based on spectral symmetry. The calculation of the red-edge inflection wavelength ($\lambda_i$) provides a standard reference for monitoring spectral shifts between communities through time.

Second-derivative data are used to identify red-edge inflection wavelengths for Jasper Ridge communities. Second-derivative curves amplify changes in spectral reflectance slope between consecutive red-edge bands. As most vegetation exhibits increasing reflectance values between the red trough and the NIR plateau, the first- ($\rho'$) and second-derivative ($\rho''$) transformations emphasize subtle absorption/reflection features as deviations along the otherwise near-linear central red-edge. Deriving red-edge spectra as single values reduce spectral data and generate a time-series. Identifying red-edge spectral shifts through derivative analysis permits the comparison of seasonal intra- and inter-community change.

Second-derivative calculations define $\lambda_i$ as the wavelength where $\rho''$ values cross zero. The identification of $\lambda_i$ enables the tracking of wavelength displacements through time as spectral shifts. Red-shifts denote changes to longer wavelengths and blue-shifts to shorter wavelengths. Spectral shifts of $\lambda_i$ can be correlated to changes in leaf chlorophyll concentrations, leaf area index, leaf inclination angle, moisture deficit stress, heat stress, and changes in other environmental factors (Guyot *et al.*, 1992; Merton *et al.*, 1997).

## 2.2 Red-edge Vegetation Stress Index

The application of second-derivative spectral analysis in this study permitted the identification of anomalous community red-edge reflectance spectra not conforming to established descriptions of an asymptote shape. Red-edge reflectance spectra for vegetation generally exhibit concave lower red-edge curves and convex upper red-edge curves. However, calculations and plots of first- and second-derivative data show spectral anomalies in upper red-edge curve shape. A critical "break-point" was identified occurring mid-way (~0.716μm) along the red-edge. Below this mid-point, red-edge curves displayed predominantly concave shapes with lower geometric

variability. At longer wavelengths beyond the break-point, curves either: *1.* displayed increasing reflectance (nominal "asymptote curve"), *2.* continued as near-linear curves (anomalous "near-linear curve"), or *3.* exhibited decreasing reflectance followed by a marked increase (strongly anomalous "cuspoid curve"). Additionally, the degree of concavity for each community appeared to vary over time in response to changes in environmental stress. Comparisons with radiance data confirmed that these features were not an artifact of user error or reflectance calibration. Further analysis showed that anomalous spectra were not restricted to one or two datasets, nor to a distinct "data year".

The Red-edge Vegetation Stress Index (RVSI) was developed in this study to identify inter- and intra-community trends based on spectral changes in upper red-edge geometry. The RVSI derives measures of spectral concavity as a displacement in reflectance between a "modeled" linear mid-point (defined as the mean reflectance of two bisecting points; the red-edge break-point (~0.716μm) and the start of the NIR plateau) and the "data" mid-point value. The difference between the two modeled and data mid-point values can then be expressed as positive or negative values. The RVSI is defined as:

$$RVSI = \left( \frac{\rho_{714} + \rho_{752}}{2} \right) - \rho_{733}$$

**Equation 1 Red-Edge Vegetation Stress Index**

*where:* ρ = reflectance at wavelength centers (nm)

Concave curves produce positive displacements from the data mid-point to the modeled mid-point value position (Figure 1). As this index is designed to measure stress, positive index values indicate increased degrees of relative stress. Conversely, negative index values are calculated for convex upper red-edge curves. A zero value marks a probable transition between stressed and non-stressed values. Figure 1 illustrates examples of convex and concave upper red-edge spectra.

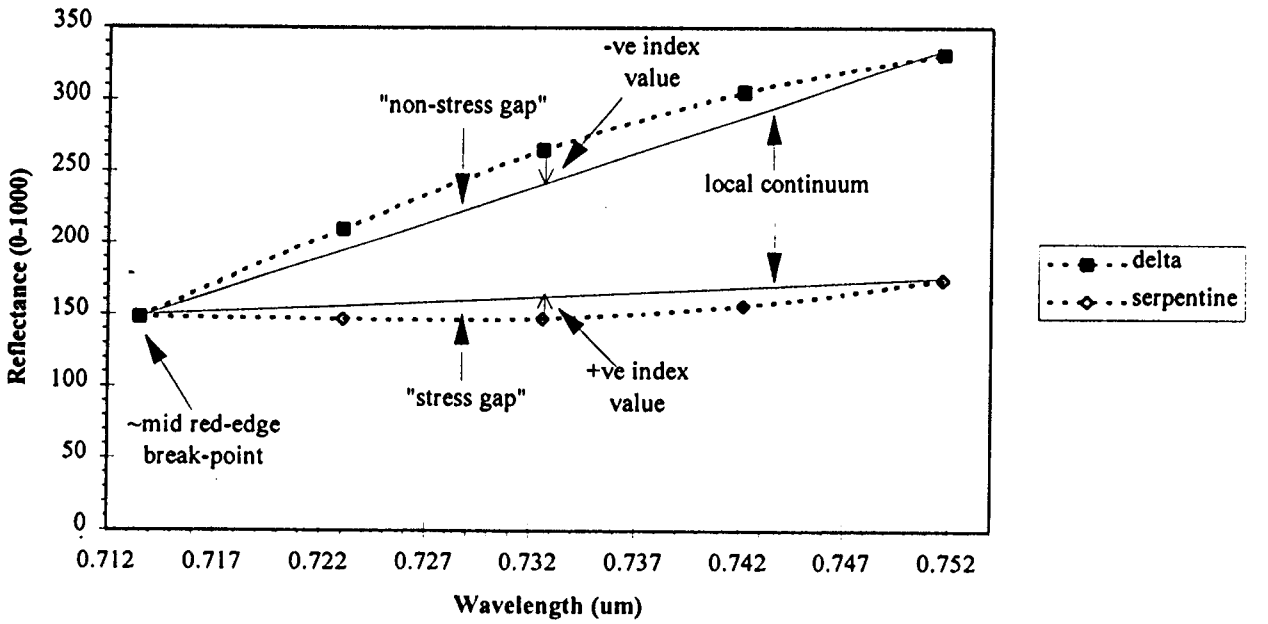


**Figure 1 Upper Red-Edge Spectra For The "Low Stress" Delta Community (30 April) And "High Stress" Serpentine Community (1 September).** *Note:* examples are selected to illustrate convex (non-stress) and concave (stress) curve shapes.

In Figure 1, the stress/non-stress "gaps" indicate the area under or over the max. - min. bisect line. An "area under the curve" integration could also be applied as an alternate measure of stress. However, the RVSI is designed to be sensitive to data variations by calculating reflectance shifts near the point of maximum displacement. Secondly, the RVSI does not directly incorporate measurements from the two data tails, which more closely fit the modeled linear min-max relationship. Thirdly, this research aims to produce a simple index that can be readily interpreted. Particular emphasis is given in this paper to the interpretation of RVSI multi-temporal trends.

## 2.3 Red-Edge Hysteresis

This component of the research attempts to plot data values as multi-temporal hysteresis trends to gain an understanding of the seasonal dynamics of calculated red-edge parameters as discrete intra- and inter-community patterns. By plotting two variables against each other, subtle seasonal hysteresis relationships can be readily interpreted.

Hysteresis is a form of analysis commonly used in geology to model multi-event data. Hysteresis is a term 'borrowed from the study of magnetism and used to describe a bivariate plot, which evidences a looped form' (Goudie, 1994, p269). In a simple elastic hysteresis event, forces act on an body causing data values to displace along a trajectory. The subsequent removal of forces may produce a return to the original values along the reciprocal or an alternate cyclic trajectory path. The direction of cyclic hysteresis is commonly described as either clockwise or anti-clockwise.

Plotting patterns of hysteresis between data points is achieved through the application of 'exponential smoothing'(Microsoft, 1997) to extrapolate data as spline lines. This technique predicts a value based on the forecast for the prior period, adjusted for the error in the prior forecast. Exponential smoothing uses a smoothing constant, the magnitude of which determines how strongly forecasts respond to errors in the prior forecast. Spline lines are used as "indicators only" and assist in interpretation as extrapolated trends between calculated values.

## 2.4 Vegetation Indices

A selection of five indices developed for vegetation studies are correlated with RVSI values. The indices are used in this study to identify possible associations with key biochemical and biophysical canopy parameters. The following is a brief description of indices selected.

•*Percent Lignin* (Aber and Martin, 1995): an index used to derive a canopy lignin concentration. Canopy lignin is particularly important ecological indicator as a very strong relationship exists between canopy lignin concentration and annual net nitrogen mineralisation, or nitrogen cycling.

•*Moisture Stress Index* (MSI) (Miller, Elvidge, Rock, and Freemantle, 1990): is used here to quantify the relative amount of canopy moisture in each vegetation community. The sensitivity of the MSI is related to total canopy water content. Moisture stressed canopies have a higher ratio value compared to non-stressed canopy sites.

•*Normalized Difference Vegetation Index* (NDVI): a widely used broad-band canopy greenness indicator. The NDVI is substituted with single AVIRIS wavelengths (667nm and 831nm) to form a narrow-band equivalent.

•*Percent Nitrogen* (Aber and Martin, 1995): an index to estimate canopy nitrogen concentrations from AVIRIS spectra at 764nm and 1640nm. Chlorophyll content in foliage is highly correlated with total protein, and therefore total nitrogen content. 1640nm is a first overtone of a C-H absorption band.

•*Photochemical Reflectance Index* (PRI) (Gamon, Roberts, and Green, 1995): is derived from reflectance at 531nm and 570nm from AVIRIS datasets. PRI varies with photosynthetic capacity, radiation-use efficiency, and vegetation type. Vegetation types exhibiting chronically reduced photosynthesis during periods of stress invest proportionally more in photoprotective processes than vegetation with high photosynthetic capacity.

# 3. RESULTS

## 3.1 Red-Edge Inflection From Second-Derivative Spectra

Red-edge inflection wavelength values ($\lambda_i$) calculated by the second-derivative technique for seven Jasper Ridge communities are plotted in Figure 2.

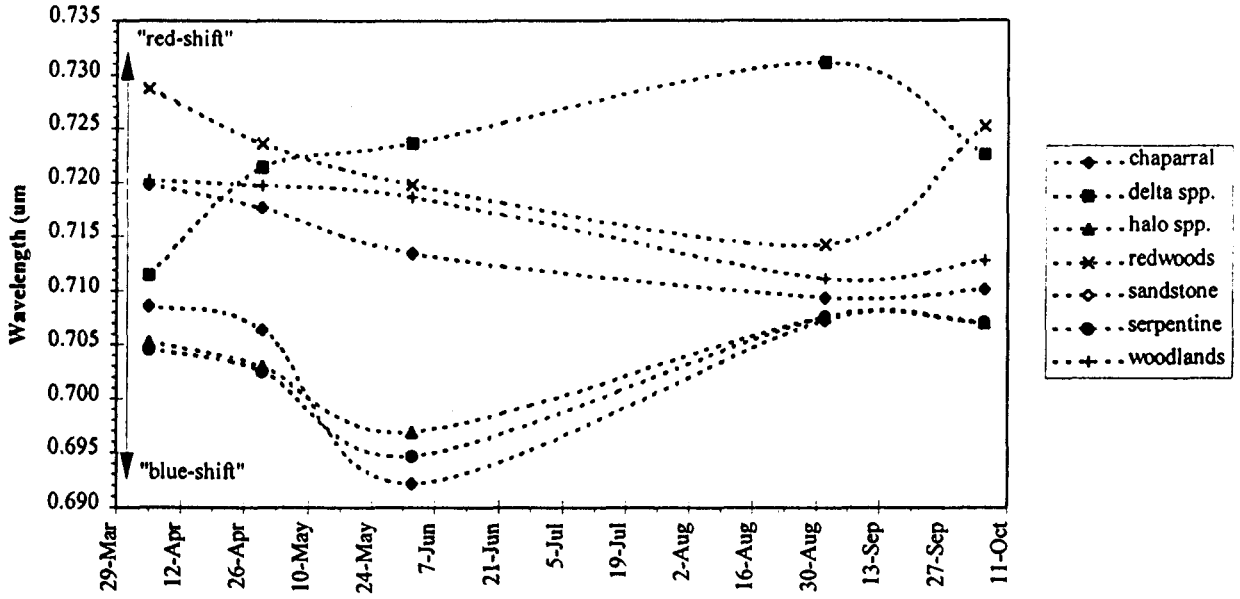


**Figure 2 Mean Community Red-Edge Inflection Wavelength Values ($\lambda_i$) Plotted As Time-Series Data.** *Note:* Spline lines between data values are exponentially smoothed to indicate data trends only.

From multi-temporal $\lambda_i$ values displayed in Figure 2, three distinct community "clusters" can be identified. The first community cluster consists of redwoods, woodlands, and chaparral communities. Figure 2 displays these communities with steadily decreasing $\lambda_i$ values from early spring to early autumn. Early autumn to late autumn is characterized by a red-shift, particularly evident in the redwood community. For these communities, a blue-shift can therefore be associated with increasing environmental stress. Additionally, late season red-shifts indicate a reduction in environmental stress associated with decreased heat and moisture deficit stress.

The second cluster contains the delta community. This community is characterized by consistently increasing $\lambda_i$ values from early spring to early autumn, interpreted as a response to increasing leaf chlorophyll and increasing LAI, a result of a seasonally high water table. The abrupt blue-shift in late autumn is likely to be a direct stress response to lowering of the water table and to the reduction in both LAI and leaf chlorophyll associated with the onset of senescence. Interestingly, the trends between the first and second clusters are reversed, indicating a strong difference between these two community clusters and their environments.

The third cluster is represented by the sandstone, halo and serpentine communities. Figure 2 displays $\lambda_i$ value trends for these communities as gradually decreasing to shorter wavelengths between early and late spring. The subsequent period to summer exhibits an abrupt increased blue-shift associated with maximum environmental stress. This stress maxima occurs earlier than first cluster communities resulting from the onset of mid summer senescence and advanced seed set. Autumn $\lambda_i$ values approximate those experienced during spring, indicating a return to lower stress conditions and the emergence of new growth.

## 3.2 Red-Edge Vegetation Stress Index

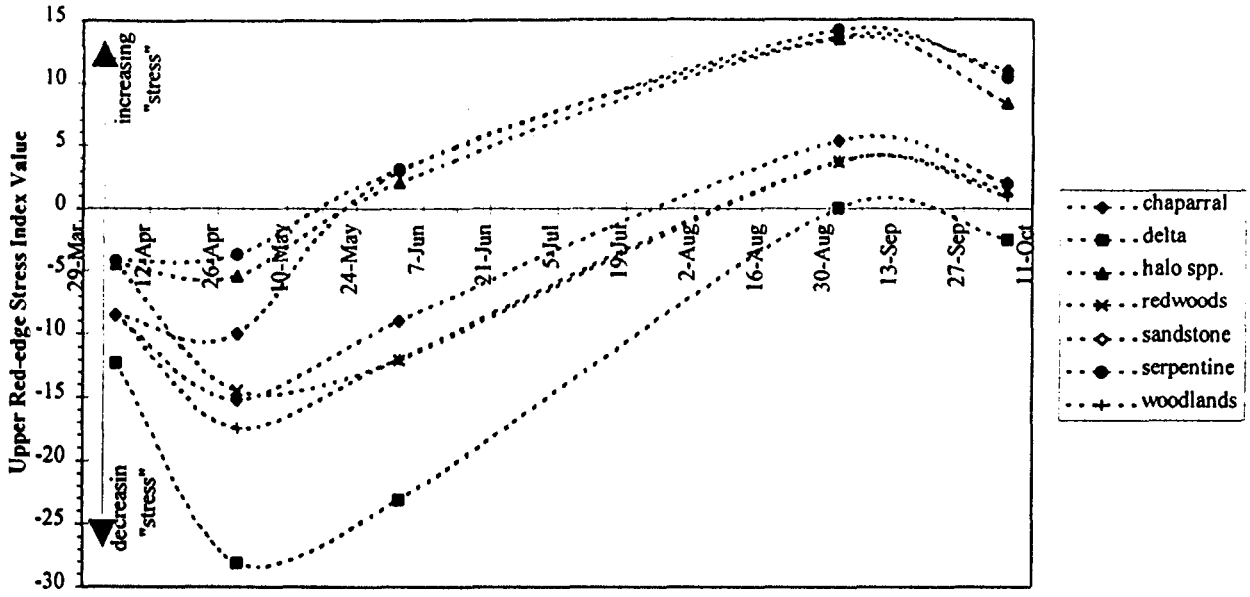


**Figure 3 Mean Community RVSI Values Plotted As Time-Series Data.** *Note:* Low stress = negative values, high stress = positive values. Spline lines between data values are exponentially smoothed to indicate data trends.

RVSI values for each community are plotted in Figure 3 to provide a graphical representation of data trends. Selected interpretations from Figure 3 are summarized as follows. All community data values on 5 April and 30 April have low stress (-ve RVSI) values. In contrast, 1 September values indicate high stress (+ve RVSI) values. Intermediate dates provide good comparative indicators for the timing and magnitude of community-specific stress. The time-series plot (Figure 3) shows decreasing RVSI values for all communities during the 5 April to 30 April period related to an early spring vigorous growth phase. Environmental conditions produce near-optimal growth conditions around 30 April resulting in lowest stress values for most communities. Data values and spline lines indicate that the peak of this optimal phase is likely to be centered in early to mid May. Community spectra shift from negative to positive RVSI values by 1 September in response to seasonal environmental stress. Positive RVSI values indicate an early onset of environmental stress for serpentine, halo, and sandstone communities occurring from mid-May.

With the onset of hot/dry summer conditions, environmental stress on plants increase. The period between 30 April and 2 June shows a general increase in RVSI values for all communities. Major differences in the rate of value change between communities is evident. The abrupt increase in RVSI values for the annual sandstone grassland community can be interpreted as early spring growth to the early onset of late summer senescence. The redwood community by contrast, shows the lowest rate of change between 30 April and 2 June, possibly reduced by the north facing microclimatic conditions.

All communities except the delta community show a similar increase in RVSI values over the period 2 June to 1 September. The delta community displays a relatively steep rate of change between the two dates becoming only marginal stressed (RVSI = 0.05) by 1 September. The period 1 September to 6 October shows decreasing RVSI values for all communities, a response to decreasing environmental stress associated with cooler autumn conditions. Total rainfall during this period is not however significantly higher than summer.

### 3.2.1 *Correlation Of RVSI Values To Selected Environmental Variables and Vegetation Indices*

Figure 4 illustrated the relationship between multi-temporal RVSI values and two important environmental variables, precipitation and temperature. The plot combines two independent sets of correlation results as a graphical summary.

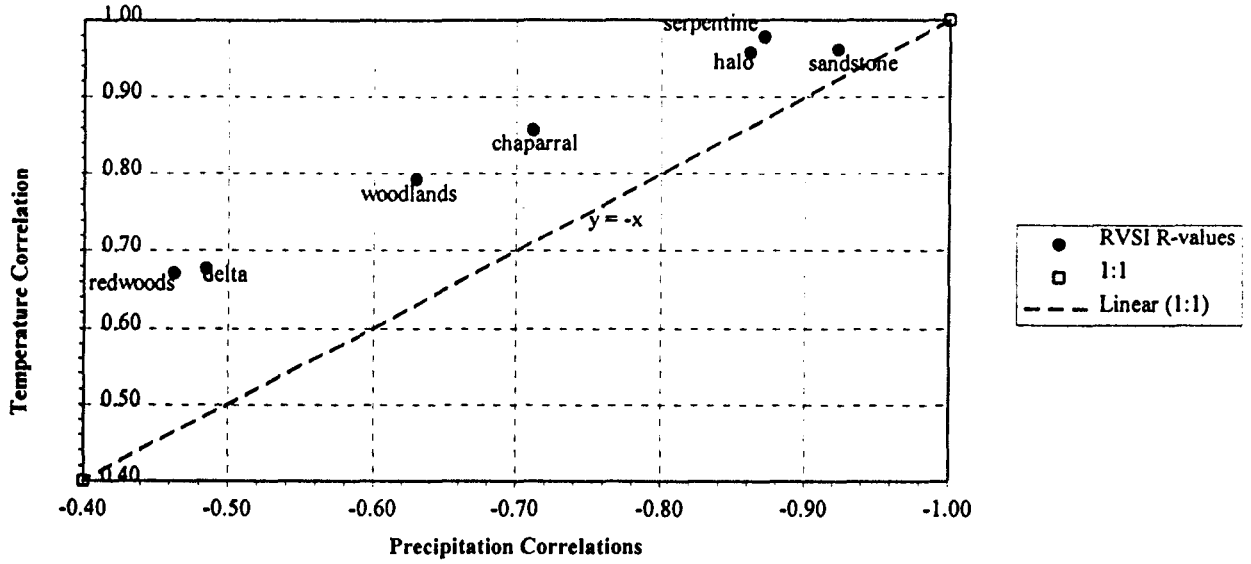


**Figure 4 Correlation Of RVSI Values To Precipitation And Temperature.** *Note:* This plot indicates the relative importance between two key environmental variables to RVSI multi-temporal correlation trends. Precipitation = daily precip, temperature = daily max. temp. Refer to Table 1 for correlation values.

Communities with high negative correlations between RVSI values and precipitation are associated with patterns of decreasing rainfall and increasing vegetation stress. Similarly, increasing temperatures indicate increasing RVSI values. A near-linear gradient of community correlation trends can be identified. A modeled linear (1:1) regression line is fitted to indicate which of the two variables is more highly correlated to RVSI value trends. Community RVSI values are more highly correlated to patterns of temperature than to precipitation.

Community correlation trends are not parallel to the linear (1:1) regression line but converge towards higher correlations. Sandstone community correlations have similar precipitation values ($R = -0.923$) and temperature values ($R = 0.962$), indicating a comparable response to both variables. Conversely, the redwood community has dissimilar precipitation ($R = -0.463$) and temperature ($R = 0.671$) correlations, indicating that this community may be more strongly influenced by temperature than precipitation. However, for communities with decreased correlation values such as redwoods and delta, this observation may be less significant.

Correlation analysis is also performed to compare RVSI values with important biochemical and biophysical indices such as percentage nitrogen (Aber *et al.*, 1995), percentage lignin (Aber *et al.*, 1995), Moisture Stress Index (MSI) (Miller, *et al.*, 1990), NDVI, and the Photochemical Reflectance Index (PRI) (Gamon, *et al.*, 1995). Correlations between RVSI and indices for each community are summarized in Table 1.

Results show that individual indices are not consistently highly correlated to RVSI values, indicating that RVSI is not a facsimile of another index. The closest consistent match for all communities exists between RVSI and NDVI, consistent with the decay of the red-edge reflectance. Similar correlation trends between communities may indicate community-specific and community clustered relationships. Community gradients can also be identified based on R value ranking. For example, MSI correlated to RVSI can be ranked to provide a community gradient:

redwoods (-0.623), delta (-0.586), woodlands (0.611), halo (0.815), chaparral (0.890), sandstone (0.891), serpentine (0.913). Community gradients can be used to compare the relative influence of biochemical and biophysical indices for each community.

**Table 1 Community Correlation Values Calculated Between RVSI And Selected Environmental Variables and Vegetation Indices.**

| *RVSI* | *Precip.* | *Temp.* | *Lign.* | *MSI* | *NDVI* | *Nitro.* | *PRI* |
|---|---|---|---|---|---|---|---|
| **chaparral** | -0.711 | 0.858 | 0.512 | 0.890 | -0.712 | -0.342 | -0.051 |
| **delta** | -0.485 | 0.677 | 0.699 | -0.586 | -0.562 | -0.790 | -0.405 |
| **halo** | -0.862 | 0.958 | -0.736 | 0.815 | -0.730 | 0.820 | -0.009 |
| **redwoods** | -0.463 | 0.671 | 0.869 | -0.623 | -0.446 | -0.869 | -0.172 |
| **sandstone** | -0.923 | 0.962 | -0.792 | 0.891 | -0.880 | 0.890 | -0.125 |
| **serpentine** | -0.872 | 0.979 | -0.734 | 0.913 | -0.730 | 0.732 | 0.076 |
| **woodlands** | -0.630 | 0.793 | 0.874 | 0.611 | -0.711 | -0.863 | -0.045 |

## 3.3 Red-edge Hysteresis

The section contains a selection of hysteresis plots followed by brief interpretations of key points. Patterns of hysteresis for red-edge inflection and RVSI are plotted against the NDVI to assist interpretation.

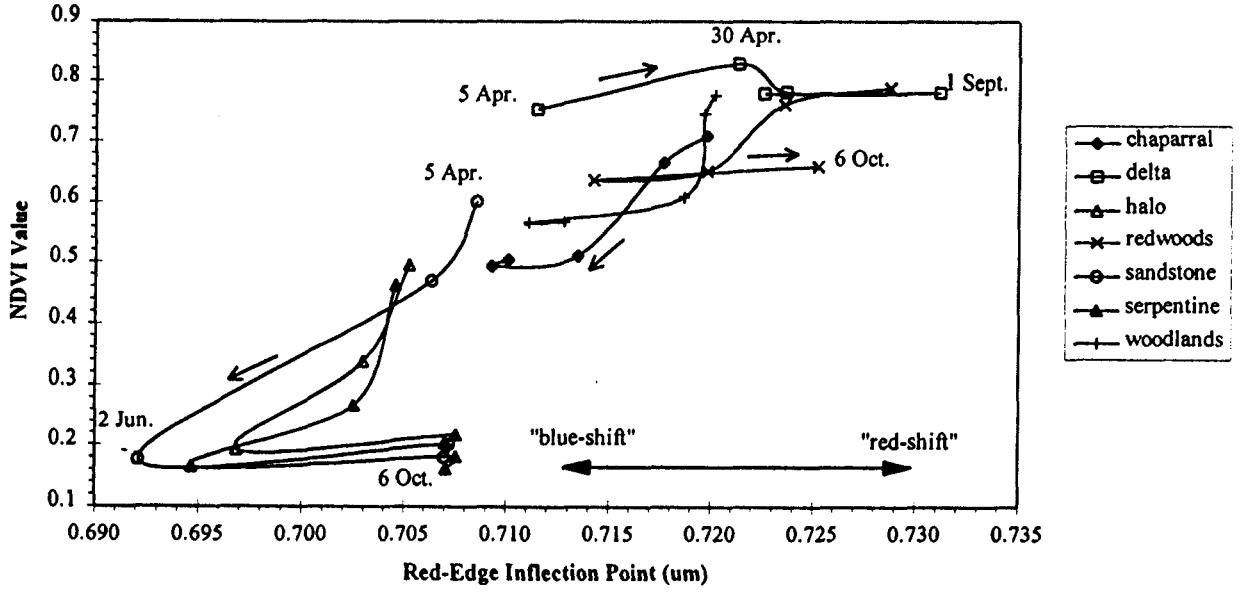


**Figure 5 Hysteresis Plot Showing The Multi-Temporal Relationship Between The Red-Edge Inflection Point ($\lambda_i$) And NDVI Values.** *Note:* arrows indicate the direction of hysteresis. Dataset dates: 5 April, 30 April, 2 June, 1 September, 6 October. Spline lines between data values are exponentially smoothed to indicate data trends. Wavelength is plotted on the x axis.

Figure 5 plots $\lambda_i$ values against NDVI in a graphical representation of temporal hysteresis trends. Note the division of tree communities from grassland and serpentine-related communities. Serpentine, halo, and sandstone, communities display a significantly blue-shift from 5 April to 2 June and a red-shift from 2 June onwards producing an anti-clockwise hysteresis. In contrast to other communities, delta displays a large red-shift from 5 April to 1 September, followed by a blue-shift to 6 October.

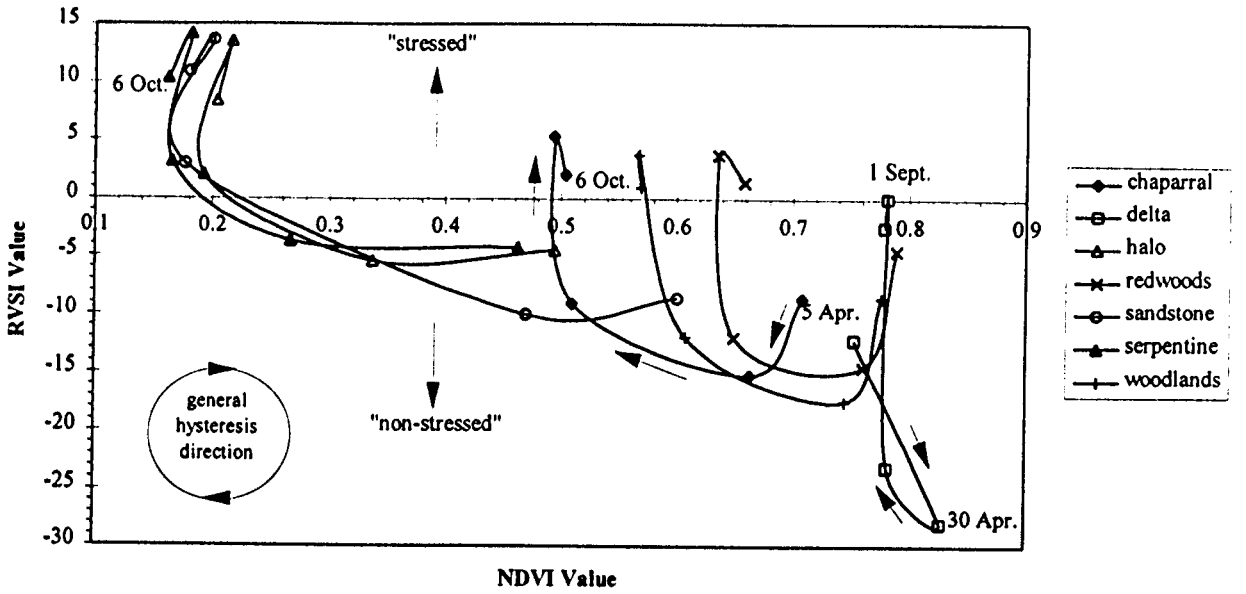


**Figure 6 Hysteresis Plot Showing The Multi-Temporal Relationship Between RVSI Values And NDVI Values.** *Note:* refer to Figure 5 for explanation.

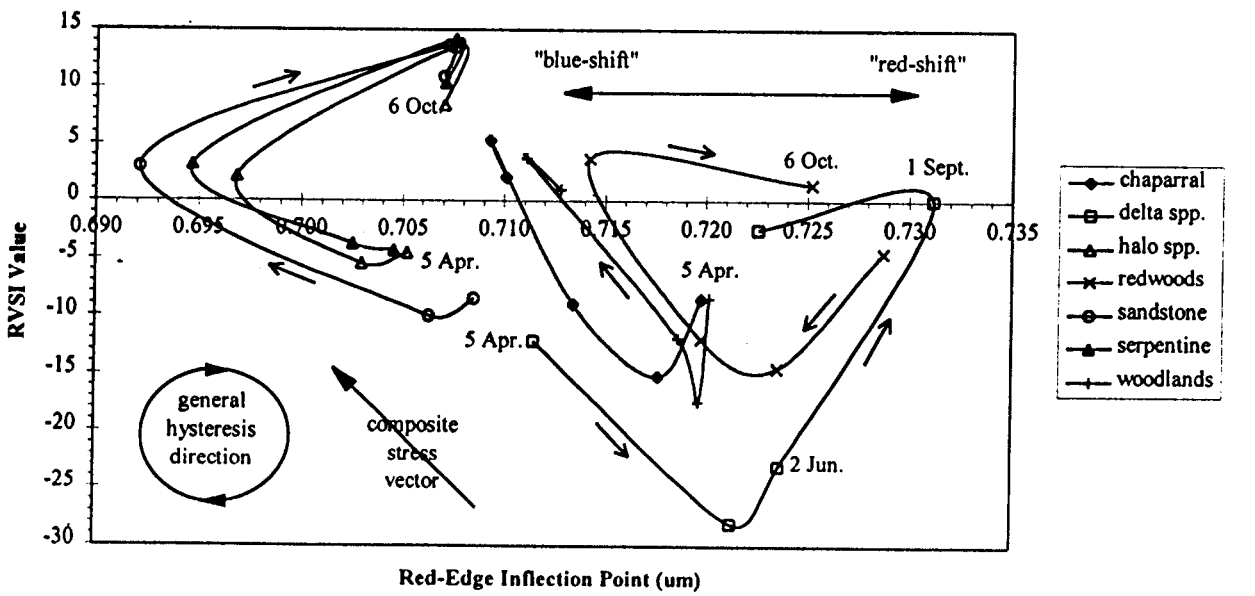


**Figure 7 Hysteresis Plot Showing The Multi-Temporal Relationship Between The Red-Edge Inflection Point ($\lambda_i$) And RVSI Values.** *Note:* refer to Figure 5 for explanation. The pattern of hysteresis for the redwoods community provides a satisfactory initial reference for interpreting trends.

Most communities in Figure 6 display a clockwise direction of hysteresis between RVSI and NDVI values. A general trend from serpentine to delta communities is evidenced by decreasing RVSI values and increasing NDVI values. Additionally, a decrease in the width of community hysteresis trajectories with increasing NDVI is also apparent along this trend.

Figure 7 combines RVSI values and $\lambda_i$ values for an assessment of two vegetation stress red-edge indicators. Patterns of multi-temporal stress hysteresis appear to be strongly cyclic. All communities except the delta community exhibit a general clockwise hysteresis. Plots identify the sandstone grassland and serpentine-related communities as disparate. RVSI and red-edge inflection appear to be indicators of distinct components of vegetation stress. The relationship between the two variables is complex.

## 4. CONCLUSIONS

This research has applied a selection of analyses including, red-edge inflection calculations, derivative spectra, RVSI values, and hysteresis plots to an assessment of vegetation community stress. Red-edge inflection and the RVSI performed well as indicators of multi-temporal stress at the community scale.

Main research findings can be summarized as follows: Asymptote and near-linear curves generally appear in early season. Cuspoid spectra are associated with mid- to late season community phenology. Upper red-edge concavity is correlated to seasonal changes in precipitation and temperature. Upper red-edge cuspoid curves become increasingly concave during periods of increasing environmental stress. The RVSI performed satisfactorily as an indicator of changing phenology and environment-induced vegetation stress. Hysteresis plots assist in the clarification of relationships between a range of red-edge measures. Community clusters can be identified from the shape and trajectory of multi-temporal hysteresis curves.

Current research focuses on the biotic and abiotic factors influencing vegetation red-edge geometry and relationships to spectral shifts. Additionally, increasing the number of datasets may improve the accuracy of mapping multi-temporal trends. Analyzing annual patterns of hysteresis may also prove a useful tool for long-term studies of environmental and ecosystem change.

## 5. REFERENCES


Aber, J.D., Martin, M.E. (1995). High Spectral Remote Sensing of Canopy Chemistry, In: *Summaries of the Fifth Annual JPL Airborne Earth Science Workshop*, Vol. 1, AVIRIS Workshop (Ed: R.O. Green), January 23-26, 1995. NASA Jet Propulsion Laboratory publication 95-1, Vol.1, p1-4.

Gamon, J.A., Roberts, D.A., Green, R.O. (1995). Evaluation of the Photochemical Reflectance Index in AVIRIS Imagery, In: *Summaries of the Fifth Annual JPL Airborne Earth Science Workshop*, Vol. 1, AVIRIS Workshop (Ed: R.O. Green), January 23-26, 1995. NASA Jet Propulsion Laboratory publication 95-1, Vol.1, p55-58.

Goudie, A, (1994). *The Encyclopedic Dictionary of Physical Geography*. Blackwell, Cambridge, Mass, 611p.

Guyot, G., Baret, F., Jacquemoud, S. (1992). Imaging Spectrometry for Vegetation Studies. In: *Imaging Spectroscopy: Fundamentals and Prospective Applications*, (Ed: Toselli and Bodechtel), Kluwer Academic Publishers, The Netherlands, 145-166.

Merton, R.N. (1994). *Hyperspectral remote sensing of environmental and biogeochemical stress at Jasper Ridge, California.* MSc.(Hons) Thesis. Department of Geography, University of Auckland, New Zealand. 135p.

Merton, R.N., Harvey, L.E. (1997). Analysis of Seasonal Changes In Jasper Ridge Vegetation Biochemistry And Biophysiology Using Multi-Temporal Hyperspectral Data. *ASPRS Conference*, Seattle, WA. 6-10 Apr 1997.

Microsoft Corporation, (1997). *Microsoft Excel, Vers. 7.0a*, Seattle WA. USA.

Miller, J.R., Elvidge, C.D., Rock, B.N., Freemantle, J.R. (1990). An Airborne Perspective on Vegetation Phenology From the Analysis of AVIRIS Data Sets Over the Jasper Ridge Biological Preserve. In: *Proceedings of the IEEE Geosciences and Remote Sensing Society/URSI 1990 Conference.*